

## Versatile platform for creating gradient combinatorial libraries via modulated light exposure

Brian C. Berry, Christopher M. Stafford, Mayur Pandya,<sup>a)</sup> Leah A. Lucas,<sup>b)</sup> Alamgir Karim, and Michael J. Fasolka<sup>c)</sup>

*Polymers Division, National Institute of Standards and Technology, Gaithersburg, Maryland 20899*

(Received 6 November 2006; accepted 18 February 2007; published online 10 July 2007)

This article details the design, construction, and operation of flexible system that modulates light exposure for the purpose of fabricating continuous and discrete gradient combinatorial libraries. Designed for versatility, the device combines “off the shelf” components, modular accessories, and flexible computer control, so that it can be used for a variety of combinatorial research applications. Salient aspects and capabilities of the instrument are illustrated through two practical examples. The first case demonstrates how user defined exposure functions can be used to create continuous surface energy gradient libraries with a linear profile. The second example illustrates the creation of continuous and discrete libraries for mapping exposure-property functions in a photocurable polymer system. [DOI: 10.1063/1.2755729]

### I. INTRODUCTION

Implementation of combinatorial and high-throughput approaches for material research hinges on the ability to fabricate appropriate specimen libraries. Depending on the research application, library creation requires systematic variation of one or more experimental variables, such as chemical factors (e.g., molecular structure and surface properties), physical variables (e.g., coating thickness and device geometry), or processing parameters (e.g., temperature and reaction time). In addition, for quantitative “combi” measurements, it is necessary to fabricate libraries in a reliable, predictable, and repeatable manner.

Designing instruments for creating combi specimen arrays can be complex and time consuming; and existing technology cannot always be leveraged toward an effective solution for a new application. Accordingly, library fabrication is often the primary barrier to implementing combi for emerging material systems. Moreover, in the case of established work flows, this challenge can reemerge when even modest changes in the research focus are necessary. Given these challenges, *versatile* library fabrication routes and instrumentation that can be easily modified and applied to a variety of applications are extremely valuable to combi researchers. The so-called gradient library fabrication approaches, which result in specimens that gradually and continuously vary one or more parameters over space, can offer this flexibility due to the relatively simple instrument designs needed to implement these techniques. For example, consider the gradient codeposition approaches that have been used extensively to fabricate libraries of inorganic materials (see, for example, Refs. 1–4 and two recent reviews<sup>5,6</sup>). Using a

straightforward, malleable instrument design, these techniques can create multivariate libraries of the wide variety of metals and oxides that can be deposited via sputtering, evaporation, or chemical vapor deposition. Continuous gradient approaches have also been developed for organic and polymeric materials, which are the focus of this article. These methods have been used to fabricate libraries of a variety of parameters, including polymer blend composition,<sup>7–9</sup> surface functionality,<sup>10–14</sup> film thickness,<sup>15</sup> and processing parameters.<sup>7,9,12,16</sup> The flexibility demonstrated by such approaches provides context and motivation for the work described here.

In this article, the design, construction, and operation of a system that modulates light exposure for the purpose of fabricating continuous and discrete gradient combinatorial libraries are detailed. The flexible system design includes a set of modular accessories for manipulating a variety of types of light sources for different applications. The versatility of this instrument is further enhanced by custom built software that can generate continuous and discrete exposure profiles according to user defined mathematical functions. This software control is essential for the reliable, reproducible fabrication of libraries that meet experimental designs. As discussed below, the gradients in radiation exposure produced by this device have the potential to create a wide range of libraries. Indeed, recent studies have demonstrated light exposure as a versatile means for fabricating gradient libraries for examining phenomenon such as substrate surface energy,<sup>13,17–19</sup> surface driven self-assembly,<sup>19,20</sup> photopolymerization,<sup>21–23</sup> photocuring,<sup>24,25</sup> and photolithography.<sup>26</sup>

To illustrate the salient capabilities of our instrument, the fabrication of two kinds of combinatorial libraries is described in this article. The first example considers the creation of continuous gradients in substrate surface energy ( $\gamma$ ),<sup>17,27</sup> which can govern the behavior and stability of overlying films,<sup>19,28–30</sup> coatings, and biosystems.<sup>31</sup> In this case,

<sup>a)</sup>Present address: Cornell University, Ithaca, New York 14850-2488.

<sup>b)</sup>Present address: Department of Chemical and Materials Engineering, Arizona State University, Phoa Arizona 85069-7100.

<sup>c)</sup>Author to whom correspondence should be addressed; electronic mail: mfasolka@nist.gov

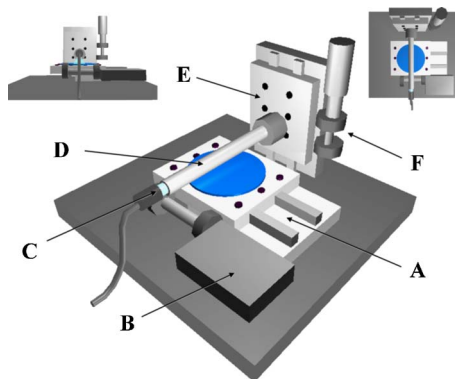


FIG. 1. (Color online) Illustration of the UVO exposure stage highlighting the sample stage (A), the actuator (B), the UV wand source (C), the wand accessory (D), the vertical translation stage (E), and the micrometer used for manual actuation of the vertical stage (E).

the device drives a graded UV ozonolysis (UVO) of molecules grafted on a substrate to create a library of surface hydrophobicity. In the second demonstration, the device is used to vary the amount of light delivered to a photopolymerizable polymer. Such libraries are useful for determining optimal processing parameters for the photolithographic fabrication of, e.g., microfluidic devices<sup>32–34</sup> and electronics.<sup>35,36</sup> In addition, details of how the accessories and software can be geared for fabrication of a variety of other libraries will be discussed.

## II. MODULATED LIGHT EXPOSURE INSTRUMENT

### A. Device design and principles

The gradient light exposure instrument has a straightforward design that can be implemented with commercially available components and a few accessories that can be custom fabricated using common machine tools. As shown in Fig. 1, the crux of the device is a one-dimensional (1D) motion stage (Newport Series 443) driven by an actuator (Newport 850F-HS, nominal resolution=0.59  $\mu\text{m}$ ). These components are used to translate a planar sample beneath a light source located in a fixed housing. Another translation stage (Newport Series 430) is arranged perpendicular to the specimen plane and is fixed in position with respect to the sample stage. This vertical stage provides a platform for mounting accessories (discussed below) used to shape the light source. The accessories are mounted via a postholder (Newport VPH-2). The height of the accessories over the sample is adjusted via a micrometer.

The light exposure profile delivered to the sample is determined via computer control of the sample stage actuator. As discussed above, the goal of our instrument is flexible library design. Accordingly, we have designed a graphical user interface (GUI) and instrument control module which allows the user to easily shape a number of parameters using National Instruments LABVIEW 7.1. Figure 2 gives an annotated image of the GUI. The GUI contains five distinct control areas. Panel A contains the jog functions for the stage. This allows the user to set the initial and zero positions of the stage and sample at any position, thus accommodating sample sizes up to 50 mm long. Start, stop, and motor ini-

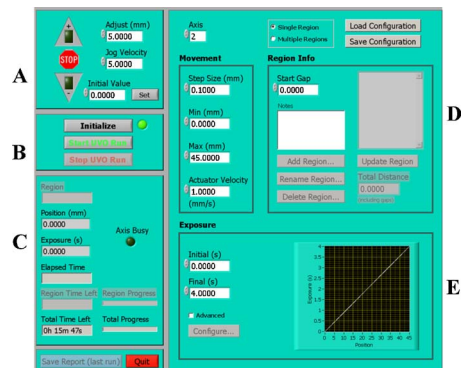


FIG. 2. (Color online) Annotated image of the designed graphical user interface (GUI) indicating panels for jog control (A); start, stop, and initialize functions (B); real time position and exposure feedback (C); actuator control (D), and exposure control (E).

tialize functions can all be found in panel B. Panel C contains the real time positional feedback as well as estimates of the elapsed and remaining times for the experiment. Sections D and E are the panels responsible for defining the movement of the stage during the experiment. Using panel D, the user can input start and end positions and the step size. In addition, the user has the ability to set a start gap (i.e., distance in front of the region of exposure over which the motor moves at full speed). Finally, the user can set the velocity of the actuator movement between steps.

This device utilizes varying wait times at each step to modulate exposure. Panel E allows the user to input profiles which define the wait time at each step (i.e. exposure to the light source). A linear profile between user defined minimum and maximum exposure times is the default profile. Exposure profiles can be made flat by setting the minimum and maximum exposures to the same value. More importantly, the control module has been designed such that the user can input any function to define a desired profile. A graphical representation of the exposure time as a function of distance traveled is provided to aid the user.

One of the major design considerations of this GUI is the ability to create regions with independent exposure profiles. When the multiple region option is selected (panel D), the user can define a number of regions across the sample and specify different exposure profiles for each region. The configuration can save and reload at a later time to simplify the experimental process.

### B. Accessories for light modification

A number of accessories for the device were designed to modify and shape a variety of light sources. These modular accessories are mounted on the vertical translation stage as described above so that they can be raised and lowered with respect to the sample via the micrometer. Accessories were designed for both wand and flood sources.

The first set of accessories is used for the so-called “wand” sources (see Fig. 3) that consist of a long, linear bulb. These sources can be acquired in a variety of UV wavelengths and dimensions (e.g., Double-Bore®, Jelight Company Inc., Irvine, CA). The source simply slides into the accessory and is secured via a set screw. The wand accesso-

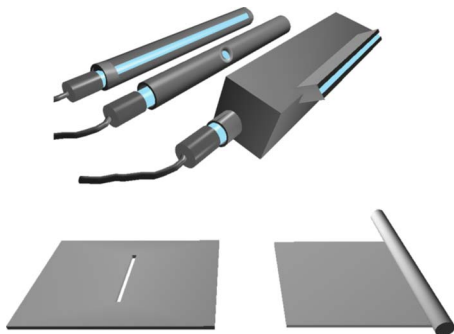


FIG. 3. (Color online) Accessories which are available for the wand sources include a slit accessory (top left), a hole accessory (top middle), and a slit collimator (top right). Accessories which are available for the flood sources include a slit mount (bottom left) and a ledge shutter (bottom right).

ries include a slit source, a hole source, and a slit collimator. The slit source (Fig. 3, top left) is a 114 mm long aluminum tube [12 mm inner diameter] with a slit of 2 mm wide cut into one side (width and length can be tailored for various samples). This appliance is good for applications where some confinement of the light is needed, but proximity to the bulb is also important. A good example is graded UV ozonolysis of the sample (discussed below) since ozone is only generated within 5 mm of the bulb face. As a result of the large slit size, the bulb must be close to the sample (<1 mm, typically, 200–500  $\mu\text{m}$ ) for effective light confinement.

The hole source (Fig. 3, top middle) is an aluminum tube with the same dimensions as the slit source except that the slit has been replaced by a 2 mm diameter drilled hole. This appliance is useful for processes which require ozone generation but which also require lateral confinement of light, for example, to produce multiple exposure libraries on the same substrate. This design could easily be extended to include an accessory with multiple holes to provide striped libraries.

The slit collimator (Fig. 3, top right) is also a useful accessory for some applications. The wand is housed in a diamond shaped tube with a slit channel along one of the vertices. The slit in this appliance is 100 mm long, 25 mm deep, and 1 mm wide. Collimation of the source is improved as a result of the deep slit channel and the reflective planes in the diamond shaped body. This tool is especially useful for libraries where light confinement is more important (e.g., lithography). In addition, the slit channel serves to separate the source from library such that proximity effects (i.e., ozonolysis) do not occur. Graded UV aging and cross-linking without ozonolysis are two examples of libraries that can be created using this accessory.

The second set of accessories also shown in Fig. 3 is used for “flood sources” (e.g., common round or flood bulbs with or without reflectors, and plane sources). A large variety of these sources in UV, visible, and IR wavelengths are available commercially, which can be harnessed for the creation of a multitude of library types. The accessories are designed to distribute such sources in a gradient fashion.

The first of the flood accessories is a slit aperture (Fig. 3, bottom left). This is a stationary opaque of  $115 \times 115 \text{ mm}^2$  panel which contains an open region ( $1.5 \times 75 \text{ mm}^2$ ) where a

slit can be mounted. The accessory can be brought within close proximity of the sample moving below it. The aperture can accept a variety of slit sizes and lengths (even points/holes). These slits can be machined into metal or even printed on transparency film.

The second flood source (Fig. 3, bottom right) accessory is a ledge shutter. This accessory consists of a stationary half-plane that can be brought into close proximity of the sample. Stage motion gradually reveals or hides the sample beneath the plate, so the exposure function is integrated over all uncovered areas. As a result, the ledge works well for two cases: (1) where a large range of exposure (very high to very low) needs to be screened in a single specimen and (2) where the creation of a library in a short amount of time is required.

As the discussion thus far illustrates, combining different light sources, appropriate accessories, and a flexible GUI, the gradient light exposure device described can be used to create a large number of libraries for a variety of combi applications. In the following sections, the versatility of the instrument will be demonstrated with two example systems. First it will be shown how an UV wand source and the slit source accessory can be used to create continuous “surface energy” or “hydrophobicity” gradient libraries. In this case, the utility and necessity of more sophisticated, flexible, and user defined sample stage motion functions using the “single region” function in the instrument control module will be demonstrated for creating well behaved libraries. Second, the use of a flood source along with the slit aperture accessory to design and fabricate libraries for processing a photopolymerized polymer system will be demonstrated. In this second case, the use of the “multiple region” function to create discrete gradient samples will be emphasized.

### III. EXAMPLE 1: SURFACE ENERGY LIBRARIES

Surface energy ( $\gamma$ ) plays an important role in a variety of polymer thin film applications. Adhesion of films to a substrate as well as the morphology of polymer blends and block copolymers are some examples of systems that are greatly affected by  $\gamma$ .<sup>37,38</sup> For example, recent studies with block copolymers have shown that particular “neutral” surface energies can result in nanostructures oriented normal to the substrate which are difficult to achieve via alternative methods.<sup>19</sup> These neutral surface energies were discovered only as a result of combinatorial methods, utilizing gradients in  $\gamma$ .

A more detailed protocol for creating surface energy libraries can be found elsewhere.<sup>13</sup> In short, a self-assembled monolayer (SAM) of octyldimethylchlorosilane (ODS) was deposited onto a clean silicon wafer via vapor deposition under low vacuum overnight. The wafers were then exposed to UVO via the wand source (Jelight 78-2096-7) housed in the slit accessory. Upon exposure to UVO, the SAM undergoes dose dependent oxidative degradation resulting in oxygen containing moieties in the exposed regions.<sup>17</sup> These moieties increase the surface energy of the SAM layer.

For this experiment, the single region function described in the GUI discussion was used. The slit accessory was set at 1.5 mm above the sample surface using the micrometer, and

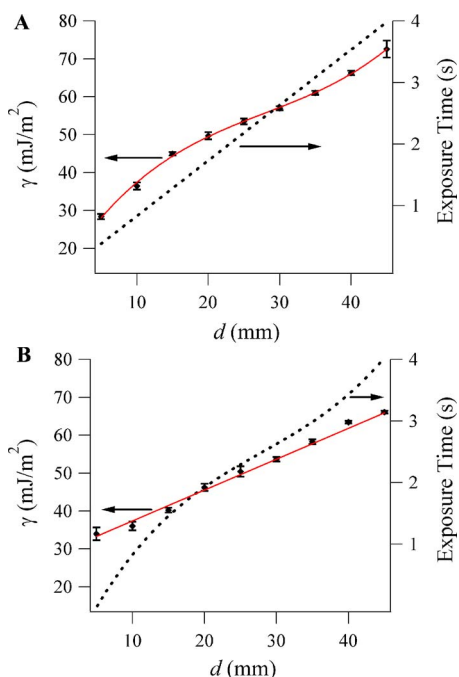


FIG. 4. (Color online) (a) Plot of the surface energy ( $\blacklozenge$ ) as a function of position resulting from a linear exposure function (---). A polynomial was used to obtain the best fit to the data (—). (b) Plot of the surface energy ( $\blacklozenge$ ) as a function of position resulting from a sigmoidal exposure function (---). A linear fit was used to obtain the best line through the data (—).

the exposure time was set using the GUI to a linear function with a minimum exposure of 0 s and a maximum exposure of 4 s. The step size and actuator velocity were set at 0.1 mm and 4 mm/s, respectively. The total distance of travel was set at 45 mm.

To quantify  $\gamma$  along the gradient, water contact angles ( $\theta_w$ ) were measured using a Krüss G2 automatic contact angle measurement system. Droplets of water were placed on the sample at 5 mm intervals.  $\theta_w$  was calculated using a Young-Laplace fit of the droplet. Multiple measurements were made at each spot. The contact angle was then converted to surface energy using the measured  $\theta_w$  and previously obtained measurements of the dispersive components of analogous systems.<sup>17,19</sup>

As demonstrated in Fig. 4 linear exposure profiles most often do not result in linear gradations in  $\gamma$ . Figure 4(a) is a plot of the  $\gamma$  along the prepared gradient ( $\blacklozenge$ ) using a linear exposure function (---).<sup>39</sup> As evident in the plot, the gradient produced deviates considerably from the linear input function. Indeed, a best fit curve analysis (—) shows that the library profile is well described by a third degree polynomial. However, in many cases, a “well behaved” linear  $\gamma$  gradient is desired. As described next, the ability to input a custom motor control function enables a user to correct for this non-linearity. Rectification of the library was accomplished in two steps. First, using the measured best fit curve from the data in Fig. 4(a), a curve was generated using the following equation:

$$g'(x) = 2f(x) - g(x),$$

where  $g'(x)$  is the function describing the curve,  $f(x)$  is the function describing the desired gradient, and  $g(x)$  is the func-

tion describing the measured values. A sigmoidal function was used to obtain the best fit to the calculated curve giving

$$g'(x) = 50.895 + \frac{46.141}{1 + e^{(28.149-x)/8.4819}}.$$

This new curve (which is in terms of  $\gamma$ ) is proportional to the exposure time needed to obtain the desired  $\gamma$  gradient. Therefore to obtain meaningful exposure values,  $g'(x)$  was scaled so that the range of exposure times defined in the original experiment was obtained. The new exposure curve which was input into the control module can be defined by the function

$$g''(x) = A(g'(x)) - c,$$

where the scaling parameters  $A$  and  $C$  equal 0.09 and 2.5, respectively. Figure 4(b) is a plot of the new exposure curve (---) ( $g''(x)$ ) and the measured  $\gamma$  along the gradient ( $\blacklozenge$ ) as a function of distance. The line fitted to the measured  $\gamma$  values (—) has a correlation value of 0.998. This demonstrates that despite the complex relationship between exposure and final library properties, a more well behaved “linear” library can be designed using the flexible GUI of this instrument and the process described above. Of course, to achieve this rectification, quality measurements of the library properties and a refining round of library fabrication are required.

#### IV. EXAMPLE 2: PHOTOPOLYMERIZABLE RESINS

The second demonstration of the gradient exposure instrument shows how it can be used to create combinatorial libraries that relate exposure dose to properties of photocurable resins. Photocurable polymeric materials are ubiquitous in industrial applications such as solventless coatings, radiation-cured adhesives, and UV-curable inks,<sup>40,41</sup> largely due to environmental and efficiency factors such as lower volatiles, faster cure times, and lower energy consumption. Photocurable materials have also been employed in technologies such as microfluidics and microelectromechanical systems (MEMS),<sup>42</sup> photolithography,<sup>43</sup> electronic packaging,<sup>44</sup> and rapid prototyping.<sup>45</sup> In all of these applications, precise control of exposure dose is critical in achieving the degree of cure, which in turn controls properties such as hardness, heat resistance, electrical conductivity, solvent resistance, and dimensional stability. Accordingly, high-throughput screening of exposure dose would enable researchers to rapidly optimize UV-curable formulations and map processing-performance relationships. Additionally, such an instrument could also provide a facile route to fabricating microfluidic devices with graded channels and components.

As a model case, a UV-curable resin, NOA 81 (Norland Products, Cranbury, NJ), was examined. NOA 81 is a multifunctional thiolene resin that is marketed as an optical adhesive but also has been used to prepare microfluidic devices and masters.<sup>33,46</sup> This model system was chosen since it cures through a frontal photopolymerization mechanism,<sup>21,47,48</sup> is not inhibited by air, and forms an excellent bond to glass. Frontal photopolymerization allows for accurate control of feature height by tuning the exposure dose and, conversely, allows for direct visualization of exposure dose by measuring the feature height. In these experi-

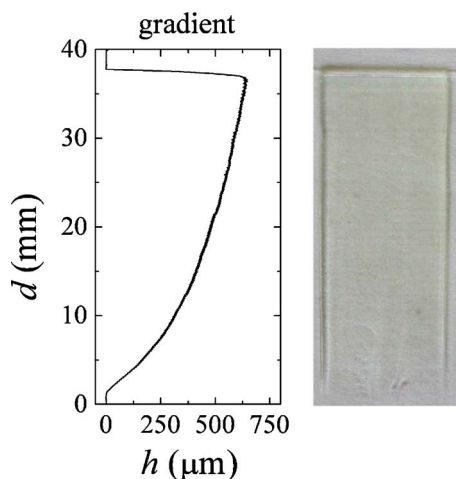


FIG. 5. Image and corresponding height profile for a continuous gradient in UV exposure of a model photocurable resin. The aperture width was 0.2 mm and the step size was 0.2 mm.

ments, the resin was placed between two glass slides separated by a silicone gasket (thickness  $\approx 1.5$  mm). To create a graded exposure library, the slit aperture accessory shown in Fig. 3 was used in conjunction with a flood UV source. The UV lamp (Spectroline SB-100P, Spectronics, Westbury, NY) had a nominal wavelength of 365 nm and an intensity of approximately  $6000 \mu\text{W}/\text{cm}^2$ , as measured by a dosimeter. The aperture was a 0.2 mm wide slit printed on a transparency. The lamp was positioned 8 cm above the slit. Three representative samples were produced using this flood source geometry: one continuous gradient specimen and two step gradient specimens.

For preparing a continuous gradient in exposure dose, the single region function of the GUI interface was used to create a linear gradient in exposure time, similar to the SAM degradation example. In this demonstration, the step size was 0.2 mm and the exposure profile was programmed to be a linear function with an initial exposure of 0 s and the final exposure of 12 s. After exposure, the top glass slide with the bonded photocured materials was lifted off the silicone gasket and rinsed with acetone to remove uncured material. The resulting library was characterized using profilometry to reveal the extent of polymerization. The height of polymerized material was measured using a Dektak 6 stylus profilometer with a stylus diameter of  $12 \mu\text{m}$ . Figure 5 shows an optical image and corresponding height profile for the gradient specimen. The most evident feature of the height profile is that the linear exposure function results in a logarithmic height profile for this model system, in agreement with previous results.<sup>46</sup> With this knowledge of the reaction kinetics, one could deduce and construct a corrected exposure profile to generate a linear height profile, similar to what was demonstrated above for surface energy gradients. One can also combine multiple graded regions to create more complex cure profiles.

In some cases, a gradient function may not provide adequate area or footprint of uniform exposure dose for subsequent analytical techniques such as IR spectroscopy, mechanical analysis, or adhesion tests to quantify the reaction process. Consequently, a step gradient in exposure dose

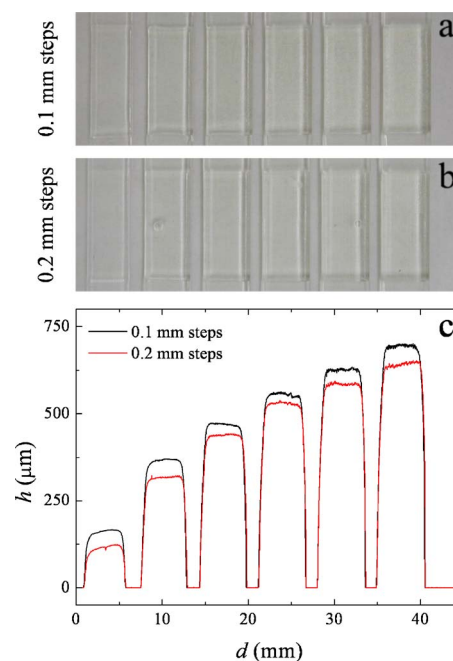


FIG. 6. (Color online) Images corresponding height profiles for discrete step gradients in UV exposure of a model photocurable resin with two different step sizes of (a) 0.1 mm and (b) 0.2 mm. The aperture width was 0.2 mm and the step size was 5 mm separated by 2 mm gaps. (c) An overlay of the height data for both step sizes of 0.1 and 0.2 mm illustrates differences in height that might be attributed to beam divergence at each step, resulting in a higher integrated exposure time for the smaller step size.

would be more appropriate. To demonstrate the ability of this instrument to create step gradients, two samples were prepared with discrete steps in exposure time using the multiple region function. Each region is programmed for uniform exposure by setting the initial and final exposure times to the same value. In the first sample, six regions of increasing exposure time were created in the GUI interface ranging from 2 to 12 s in 2 s increments with a step size within each region of 0.2 mm (equal to the aperture width). Each region was 5 mm long separated by 2 mm gaps. The gaps serve to assist in leveling the profilometry data for accurate height measurements. Additionally, the exposure times in this discrete gradient exposure function are similar to the exposure function employed above to create the continuous gradient profile. In the second sample, the step size within each region was changed in relation to the slit width, keeping the total exposure time in each region equivalent. Hence, the same six regions were created but with increasing exposure times ranging from 1 to 6 s in 1 s and a step size within each region of 0.1 mm (half the aperture width). Figure 6 shows optical micrographs (top) and height profiles for these two samples. A key feature of the data is that the feature heights in the step gradient samples are identical to the heights of the continuous gradient sample at the same exposure times. The height profiles in the step gradients also display a logarithmic growth rate akin to the continuous gradient specimen.

Our experiments reveal an important effect of the slit width on this system. The total *programed* exposure time was equivalent between the two samples, as set by the step size and exposure time at each step. However, the height data (Fig. 6) show a noticeable difference between the two

samples, with the 0.1 mm step size specimen being taller than the 0.2 mm step size. This can be attributed to the broadening of the beam after passing through the slit aperture. With smaller step sizes, the cumulative exposure outside the slit width is greater, and thus the total *integrated* exposure time at each step is higher. The beam divergence leads to higher conversions of the model resin and consequently taller structures when the step size is decreased. Indeed, this facet of the instrument performance is likely too subtle to be observed in the UVO degradation of SAM experiment due to the drop size/sampling area of water contact angle measurements.

## ACKNOWLEDGMENTS

One of the authors (B.C.B.) thanks the National Research Council Post-doctoral Fellowship program for support. Another author (L.A.L.) thanks the support of the Bell Labs Graduate Research Fellowship Program and Professor Ghassan E. Jabbour. This work made use of facilities in the NIST Combinatorial Methods Center. Certain equipment, instruments, or materials are identified in this article in order to adequately specify the experimental details. Such identification does not imply recommendation by the National Institute of Standards and Technology nor does it imply that the materials are necessarily the best available for the purpose. This is an official contribution of the National Institute of Standards and Technology, and is not subject to copyright in the United States.

- <sup>1</sup>I. Takeuchi, H. Chang, C. Gao, P. G. Schultz, X. D. Xiang, R. P. Sharma, M. J. Downes, and T. Venkatesan, *Appl. Phys. Lett.* **73**, 894 (1998).
- <sup>2</sup>P. G. Schultz and X. D. Xiang, *Curr. Opin. Solid State Mater. Sci.* **3**, 153 (1998).
- <sup>3</sup>J. S. Wang, Y. Yoo, C. Gao, I. Takeuchi, X. D. Sun, H. Y. Chang, X. D. Xiang, and P. G. Schultz, *Science* **279**, 1712 (1998).
- <sup>4</sup>X. D. Xiang *et al.*, *Science* **268**, 1738 (1995).
- <sup>5</sup>J. C. Zhao, *Prog. Mater. Sci.* **51**, 557 (2006).
- <sup>6</sup>I. Takeuchi, R. B. van Dover, and H. Koinuma, *Mater. Res. Bull.* **27**, 301 (2002).
- <sup>7</sup>J. C. Meredith, A. Karim, and E. J. Amis, *Macromolecules* **33**, 5760 (2000).
- <sup>8</sup>J. C. Meredith, A. Karim, and E. J. Amis, *MRS Bull.* **27**, 330 (2002).
- <sup>9</sup>J. W. Gilman, *J. Mater. Sci.* **38**, 4451 (2003).
- <sup>10</sup>M. R. Tomlinson, R. R. Bhat, and J. Genzer, *Abstr. Pap. - Am. Chem. Soc.* **230**, U4004 (2005).
- <sup>11</sup>C. Xu, T. Wu, J. D. Batteas, C. M. Drain, K. L. Beers, and M. J. Fasolka, *Appl. Surf. Sci.* **252**, 2529 (2006).
- <sup>12</sup>S. Chattopadhyay and J. C. Meredith, *Meas. Sci. Technol.* **16**, 128 (2005).
- <sup>13</sup>D. Julthongpiput, M. J. Fasolka, W. H. Zhang, T. Nguyen, and E. J. Amis, *Nano Lett.* **5**, 1535 (2005).
- <sup>14</sup>F. Turcu, G. Hartwich, D. Schafer, and W. Schuhmann, *Macromol. Rapid Commun.* **26**, 325 (2005).
- <sup>15</sup>C. M. Stafford, K. E. Roskov, T. H. Epps, and M. J. Fasolka, *Rev. Sci.*

- Instrum.* **77**, 023908 (2006).
- <sup>16</sup>R. A. Potyrailo and L. Hassib, *Rev. Sci. Instrum.* **76**, 062225 (2005).
- <sup>17</sup>S. V. Roberson, A. J. Fahey, A. Sehgal, and A. Karim, *Appl. Surf. Sci.* **200**, 150 (2002).
- <sup>18</sup>A. Sehgal, V. Ferreiro, J. F. Douglas, E. J. Amis, and A. Karim, *Langmuir* **18**, 7041 (2002).
- <sup>19</sup>A. P. Smith, A. Sehgal, J. F. Douglas, A. Karim, and E. J. Amis, *Macromol. Rapid Commun.* **24**, 131 (2003).
- <sup>20</sup>S. Ludwigs, K. Schmidt, C. M. Stafford, E. J. Amis, M. J. Fasolka, A. Karim, R. Magerle, and G. Krausch, *Macromolecules* **38**, 1850 (2005).
- <sup>21</sup>J. T. Cabral and J. F. Douglas, *Polymer* **46**, 4230 (2005).
- <sup>22</sup>S. Lin-Gibson, F. A. Landis, and P. L. Drzal, *Biomaterials* **27**, 1711 (2006).
- <sup>23</sup>V. S. Khire, D. S. W. Benoit, K. S. Anseth, and C. N. Bowman, *J. Polym. Sci., Part A: Polym. Chem.* **44**, 7027 (2006).
- <sup>24</sup>R. A. Potyrailo, and J. E. Pickett, *Angew. Chem., Int. Ed.* **41**, 4230 (2002).
- <sup>25</sup>R. A. Potyrailo, D. R. Olson, G. Medford, and M. J. Brennan, *Anal. Chem.* **74**, 5676 (2002).
- <sup>26</sup>B. J. de Gans, *J. Comb. Chem.* **8**, 228 (2006).
- <sup>27</sup>M. K. Chaudhury and G. M. Whitesides, *Science* **256**, 1539 (1992).
- <sup>28</sup>K. M. Ashley, D. Raghavan, J. F. Douglas, and A. Karim, *Langmuir* **21**, 9518 (2005).
- <sup>29</sup>A. P. Smith, J. F. Douglas, J. C. Meredith, E. J. Amis, and A. Karim, *J. Polym. Sci., Part B: Polym. Phys.* **39**, 2141 (2001).
- <sup>30</sup>A. P. Smith, J. F. Douglas, J. C. Meredith, E. J. Amis, and A. Karim, *Phys. Rev. Lett.* **87**, 015503 (2001).
- <sup>31</sup>S. B. Kennedy, N. R. Washburn, C. G. Simon, and E. J. Amis, *Biomaterials* **27**, 3817 (2006).
- <sup>32</sup>Z. T. Cygan, J. T. Cabral, K. L. Beers, and E. J. Amis, *Langmuir* **21**, 3629 (2005).
- <sup>33</sup>C. Harrison, J. Cabral, C. M. Stafford, A. Karim, and E. J. Amis, *J. Micromech. Microeng.* **14**, 153 (2004).
- <sup>34</sup>T. Wu, Y. Mei, J. T. Cabral, C. Xu, and K. L. Beers, *J. Am. Chem. Soc.* **126**, 9880 (2004).
- <sup>35</sup>E. F. Reznikova, J. Mohr, and H. Hein, *Microsyst. Technol.* **11**, 282 (2005).
- <sup>36</sup>N. A. Kaliteevskaya and R. P. Seisyan, *Semiconductors* **35**, 226 (2001).
- <sup>37</sup>K. L. Johnson, *Proc. R. Soc. London, Ser. A* **324**, 301 (1971).
- <sup>38</sup>K. Kendall, *J. Phys. D* **4**, 1186 (1971).
- <sup>39</sup>The data in this article, in the Figures, and in the tables are presented along with the standard uncertainty ( $\sigma$ ) involved in the measurement, where the uncertainty represents one standard deviation from the mean.
- <sup>40</sup>K. Brack and J. Braddock, *Radiation-Curable Coatings, Adhesives, and Inks: Technology and Practical Applications* (Technomic, Lancaster, PA, 1999).
- <sup>41</sup>*Radiation Curing of Polymeric Materials, Acs Symposium Series 417* (American Chemical Society, Washington, D.C., 1990).
- <sup>42</sup>N.-T. Nguyen and S. T. Werely, *Fundamentals and Applications of Microfluidics* (Artech House, Norwood, MA, 2002).
- <sup>43</sup>H. J. Levinson, *Principles of Lithography*, 2nd ed. (SPIE, Bellingham, WA, 2005).
- <sup>44</sup>P. Swanson, *Assem. Autom.* **17**, 23 (1997).
- <sup>45</sup>P. K. Venuvinod and W. Ma, *Rapid Prototyping: Laser-Based and Other Technologies* (Kluwer Academic, Norwell, MA, 2003).
- <sup>46</sup>J. T. Cabral, S. D. Hudson, C. Harrison, and J. F. Douglas, *Langmuir* **20**, 10020 (2004).
- <sup>47</sup>S. K. Reddy, N. B. Cramer, and C. N. Bowman, *Macromolecules* **39**, 3673 (2006).
- <sup>48</sup>S. K. Reddy, N. B. Cramer, and C. N. Bowman, *Macromolecules* **39**, 3681 (2006).